Macroscopic distant magnon modes entanglement via a squeezed drive

Kamran Ullah, 1, * M. Tahir Naseem, 2, † and Özgür E. Müstecaplıoğlu 1, 3, ‡

¹Department of Physics, Koç University, 34450 Sarıyer, Istanbul, Türkiye
²Faculty of Engineering Science, Ghulam Ishaq Khan Institute of Engineering Sciences and Technology,
Topi 23640, Khyber Pakhtunkhwa, Pakistan
³TÜB ITAK Research Institute for Fundamental Sciences, 41470 Gebze, Türkiye
(Dated: August 29, 2023)

The generation of robust entanglement in quantum system arrays is a crucial aspect of realizing efficient quantum information processing. Recently, the field of quantum magnonics has garnered significant attention as a promising platform for advancing in this direction. In our proposed scheme, we utilize a one-dimensional array of coupled cavities, with each cavity housing a single yttrium iron garnet (YIG) sphere coupled to the cavity mode through magnetic dipole interaction. To induce entanglement between YIGs, we employ a squeezed vacuum drive, providing the necessary nonlinearity. Our results demonstrate the successful generation of bipartite and tripartite entanglement between distant magnon modes across the entire array, all achieved through a single control drive. Furthermore, the steady-state entanglement between magnon modes is robust against magnon dissipation rates and environment temperature. Our results may find applications of cavity-magnon arrays in quantum information processing and quantum communication systems.

I. INTRODUCTION

Quantum entanglement plays a pivotal role in diverse applications of quantum information processing [1], encompassing quantum cryptography [2], quantum teleportation [3], and quantum metrology [4]. It is a crucial resource for enhancing the performance of quantum devices and technologies [5]. However, preparing long-lived entangled states, especially at the macroscopic scale, becomes challenging due to inevitable interactions between quantum systems and their environments. Consequently, the quest for generating macroscopic entangled states using various physical setups has gained significant attention. In this context, steady-state entanglement between atomic ensembles has been successfully demonstrated [6–8]. Additionally, entangled states involving macroscopic systems have been reported in different setups, such as entanglement between a single cavity mode and a mechanical resonator in an optomechanical configuration [9]. Recently, experimental achievements include entanglement between two macroscopic resonators coupled to a common cavity mode through optomechanical interaction [10].

Another central challenge in harnessing entanglement to enhance various quantum tasks lies in the ability to create and distribute entanglement across large arrays of quantum systems [11–17]. One intriguing approach to address this challenge is reservoir engineering, where external control drives are employed to engineer desirable dissipative dynamics, leading the quantum system to relax into the desired quantum state [14, 18–25]. However, most reservoir engineering schemes require multiple external control fields to be applied over different elements of the quantum system array [26, 27].

In recent years, hybrid quantum systems, combining different physical subsystems, have garnered significant attention

[28–30]. Among these systems, cavity-magnon setups offer a unique platform for investigating light-matter interactions [31, 32]. In the realm of cavity quantum electrodynamics, the strong and ultrastrong coupling between magnons and photons has been increasingly studied [31, 33–37], with experimental demonstrations of these regimes [38–40]. This strong coupling opens up possibilities for exploring novel phenomena, such as the magnon Kerr effect [41], cavity-magnon polaritons [42], magnon-induced transparency [43], magnomechanically induced slow-light [44], bistability [45], exceptional points [42, 46], and nonreciprocity [47].

Recent proposals aim to realize genuine quantum effects in macroscopic magnon-cavity systems, including magnon blockade [48], magnon squeezed states [49], Schrödinger cat states [50, 51], Bell states [52], and nontrivial bipartite and multipartite entangled states [53, 54]. Of particular interest is the generation of entanglement between distant magnon modes [55], which holds promise for quantum information processing applications. However, to the best of our knowledge, existing studies have primarily focused on entangling only two magnon modes, such as entangling two YIG spheres in a single cavity via Kerr nonlinearity [56], magnetostrictive interaction [57], or applying a vacuum-squeezed drive [58, 59]. In the case of two cavities, each containing a single YIG, entanglement between the YIGs has been generated through optomechanical-like coupling [60], vacuum squeezed drive [61], or reservoir engineering [55, 62, 63]. In a recent work [64], bipartite entanglement between magnon modes is investigated in a one-dimensional array of cavities. The entanglement is generated by exploiting the coupling of the magnon modes with respect to a central giant atom via virtual photons.

Hybrid quantum magnonic systems hold great promise for efficient quantum networks [65]. Therefore, a crucial task is to establish and control entanglement between multiple magnon modes in arrays based on quantum magnonic systems. In this regard, we propose a scheme to generate entanglement between multiple yttrium iron garnet (YIG) spheres using a reservoir engineering approach with a single control drive. Precisely, our setup consists of an array of cavities, each hous-

^{*} kullah19@ku.edu.tr

[†] mnaseem16@ku.edu.tr

[‡] omustecap@ku.edu.tr

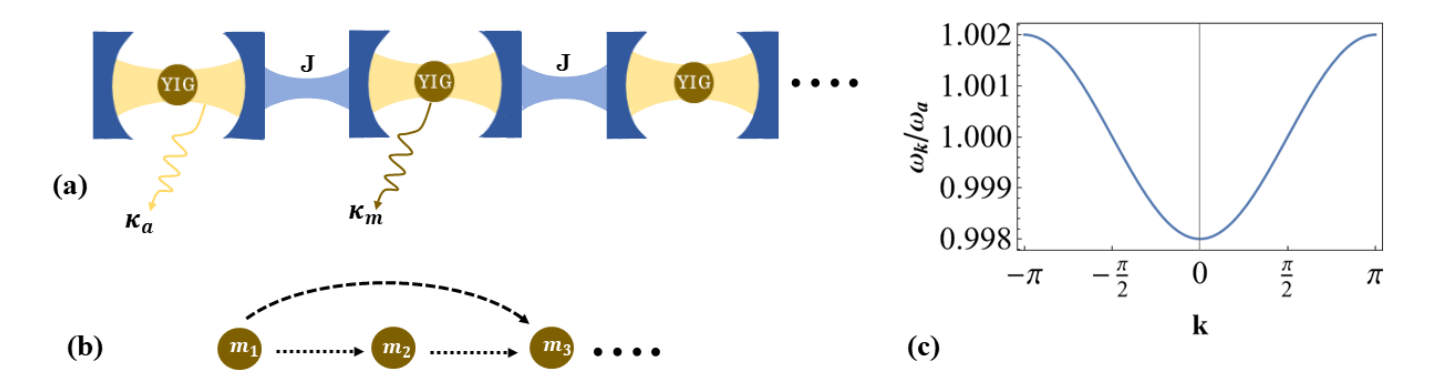


Figure 1. (a) Schematic description of magnon-magnon entanglement generation scheme, consisting of a one-dimensional 2N+1 array of identical lossy cavities coupled via hopping interaction J. Each cavity contains a yttrium iron garnet (YIG) sphere with volume V. The cavities' decay and dissipation rates are κ_a and κ_j , respectively. The central YIG in the array is driven by an external quantum squeezed drive, enabling our entanglement generation scheme. (b) Describes the effective model, which consists of only magnon modes obtained after removing the cavities via employing Schrieffer-Wolf transformation. (c) Shows the behavior of the dispersion relation of the cavity mode in momentum space.

ing a macroscopic YIG coupled to the cavity through beam splitter-like interaction. However, entanglement cannot be generated with this interaction alone; thus, we introduce the necessary nonlinearity by driving one of the magnon modes with a vacuum-squeezed drive. Previous studies have demonstrated that a single and two-mode squeezed drive can create entanglement between magnon modes [58–61]. In our work, we show that driving one of the magnon modes via squeezed drive is sufficient to generate steady-state bipartite and tripartite entanglement between magnon modes within the array of cavities.

We would like to highlight that, in principle, the input squeezed drive on the central magnon mode (m_2) can be realized by coupling an auxiliary quantum system. The generation of the squeezed input field can be accomplished using a method similar to the proposal discussed in [66]. For example, the input squeezed reservoir can be engineered by coupling an auxiliary microwave cavity to the central magnon mode through beam-splitter-type interaction. The weak squeezed vacuum field, generated via a flux-driven Josephson parametric amplifier, acts as the driving force for the auxiliary cavity. Consequently, the auxiliary cavity serves as a squeezed drive for the central magnon mode [49, 67]. Similarly, the squeezed drive can also be achieved by coupling the central magnon mode to a superconducting qubit [68]. More specifically, the approach proposed in reference [69] can be implemented by replacing the coplanar waveguide resonator with a YIG placed inside a microwave cavity. This scheme enables the coupling of a superconducting qubit with an adjustable energy gap to a magnon mode characterized by the frequency ω_2 . By modulating the energy gap of the qubit with a bichromatic field, the squeezed reservoir for the magnon mode can be engineered [49]. Alternatively, the input squeezed radiation can be generated by applying a two-tone microwave field drive to the central YIG, where the magnon mode is coupled to its mechanical vibrational mode through magnetostrictive interaction [70, 71].

The paper is structured into the following sections: In Sec. II, we introduce the model; and in Sec. III derivation of effective

Hamiltonian is presented. The results for bipartite and tripartite entanglement between the magnon modes are discussed in Secs. IV A and IV B, respectively. Finally, in Sec. V, we offer concluding remarks and summarize the key findings.

II. THE MODEL

We investigate a cavity-magnon system comprising a one-dimensional array of 2N+1 cavities, as illustrated in Fig. 1. These cavities are interconnected through photon-hopping interactions. Inside each cavity, a single YIG sphere is present, coupled to the cavity mode via magnetic dipole interaction. In this study, we consider a single magnon mode, which represents quasi-particles with collective spin excitations, associated with each YIG in the cavities. The Hamiltonian governing the field for the cavity array is as follows

$$H_a/\hbar = \omega_a \sum_n \hat{a}_n^{\dagger} \hat{a}_n - \sum_n J(\hat{a}_n \hat{a}_{n+1}^{\dagger} + \hat{a}_n^{\dagger} \hat{a}_{n+1}). \tag{1}$$

The first term represents the free energy of the cavities, while the second term accounts for the exchange energy of the field. \hat{a}_n and \hat{a}_n^\dagger are the bosonic annihilation and creation operators of the n-th cavity, and the corresponding resonance frequency ω_a . Here $n\ (n\in[-N,N])$ describes the index of the cavity in a one-dimensional array, with each cavity interconnected through a hopping coupling called J. We consider only a single photon process in each cavity. The free Hamiltonian for magnon modes is given by

$$H_m/\hbar = \sum_n \omega_n \hat{m}_n^{\dagger} \hat{m}_n, \tag{2}$$

here \hat{m}_n (\hat{m}_n^\dagger) is the annihilation (creation) operator of the magnon mode, and ω_n is the associated frequency of the mode. The interaction between the magnon and cavity modes is given by

$$H_I/\hbar = \sum_n g_n(\hat{a}_n \hat{m}_n^{\dagger} + \hat{a}_n^{\dagger} \hat{m}_n). \tag{3}$$

Here, $(\hat{m}_n \text{ and } \hat{m}_n^{\dagger})$ are the destructive and creative operators of the magnonic modes. The magnon frequencies can be calculated based on the applied magnetic fields, given by $\omega_n = \gamma H_n$, where $\gamma/2\pi=28$ GHz/T represents the gyromagnetic ratio. We note that the interaction term is obtained after performing the Holstein-Primakoff transformation in which collective spin operators are written in the form of bosonic magnon operators \hat{m} (\hat{m}^{\dagger}) [56]. In addition, the counter-rotating terms $\hat{m}\hat{a}$, $\hat{m}^{\dagger}\hat{a}^{\dagger}$ are ignored assuming the validity of rotating wave approximation [58]. In Eq. (1), g is the coupling strength and it is given by $g = \zeta \gamma / 2 \sqrt{5\hbar\omega\mu_0 N/V}$ where V is the volume of the cavity, N represents the total number of spins in the YIG, μ_0 is the permeability of free space, and ζ describes the spatial overlap between the magnon and photon modes.

THE SCHRIEFFER-WOLFF APPROXIMATION AND EFFECTIVE HAMILTONIAN

To create entanglement between two magnon modes, an effective parametric-type coupling $(\hat{m}_1^{\dagger}\hat{m}_2^{\dagger} + \hat{m}_1\hat{m}_2)$ is required. This interaction can be achieved by introducing strong Kerr nonlinearity [56] or nonlinear magnomechanical interaction [57]. However, it is more convenient to engineer an effective beamsplitter-type coupling $(\hat{m}_1^{\dagger}\hat{m}_2 + \hat{m}_1\hat{m}_2^{\dagger})$ between the magnon modes. For instance, in a system with two YIGs spheres placed inside a microwave cavity, it is possible to generate the desired coupling $(\hat{m}_1^{\dagger}\hat{m}_2 + \hat{m}_1\hat{m}_2^{\dagger})$ by carefully selecting system parameters that allow for the adiabatic elimination of the cavity mode [72]. Another approach involves an array of three cavities, where the central cavity contains a qubit, and each end cavity houses a YIG sample [63]. By employing the dispersive regime and using the Schrieffer-Wolff (Frohlich-Nakajima) approximation [73–75], the cavity modes can be eliminated, resulting in an effective beamsplitter-type coupling between the YIGs. In our case, we adopt the latter method to create an array of YIGs with an effective coherent coupling $(\hat{m}_n^{\dagger}\hat{m}_{n+1} + \hat{m}_n\hat{m}_{n+1}^{\dagger})$. The required nonlinearity for generating entanglement between distant magnon modes is achieved by driving the central YIG with a single-mode squeezed vacuum drive [66, 76–79].

The Hamiltonian H_a (Eq. (1)) associated with a onedimensional array of coupled cavities represents the tightbinding bosonic model. To diagonalize it, we introduce new operators in the momentum space (k-space). The resulting diagonal Hamiltonian is given by

$$H_{\rm diag}/\hbar = \sum_{k} \omega_k \hat{a}_k^{\dagger} \hat{a}_k, \tag{4}$$

here we have introduced

$$\hat{a}_k = \frac{1}{\sqrt{N}} \sum_n \hat{a}_n e^{-ikn},$$

$$\hat{a}_k^{\dagger} = \frac{1}{\sqrt{N}} \sum_n \hat{a}_n^{\dagger} e^{-ikn},$$
(5)

with $k \in [-\pi/a, \pi/a]$, and $\omega_k = \omega_a - 2J \cos k$ is the dispersion

relation. For convenience, we have assumed the lattice constant a=1.

To derive the effective Hamiltonian comprising only magnon modes, we must eliminate the cavity modes. To achieve this, we employ the Schrieffer-Wolf (Frohlich-Nakajima) [73, 74, 80, 81] transformation

$$[S_i, H_0] = -H_I. (6)$$

Where H_0 is the free Hamiltonian consisting of $H_{\text{diag}} + H_m$, and H_I is the interaction Hamiltonian of the system. i.e.,

$$H_m/\hbar = \sum_{j} \omega_j \hat{m}_j^{\dagger} \hat{m}_j. \tag{7}$$

$$H_I/\hbar = \sum_k \sum_j [g_k^j/\sqrt{N}(\hat{a}_k \hat{m}_j^{\dagger} e^{iklj} + \hat{a}_k^{\dagger} \hat{m}_j e^{-iklj})], \quad (8)$$

with l being the separation between two magnon modes. S_i is called a generator and it is skew-symmetric in nature i.e., $S_i = -S_i^{\star}$. The complete form of S can be expressed as

$$S = \sum_{i,k} \left[\alpha_k^i \hat{a}_k \hat{m}_i^{\dagger} - \alpha_k^{i^{\star}} \hat{a}_k^{\dagger} \hat{m}_i \right], \tag{9}$$

here
$$\alpha_k^i = \frac{g_k^i/\sqrt{N}}{\omega_i - \omega_k^-} e^{-ikx_i}$$

here $\alpha_k^i=rac{g_k^i/\sqrt{N}}{\omega_i-\omega_k^-}e^{-ikx_i}$. The effective Hamiltonian of the system can be determined by unitary transformation $e^S H e^{-S}$. Since the effective coupling α_k^i is small, therefore, we consider only second-order expansion of the unitary transformation i.e., $H_0 + 1/2[H_I, S]$, and ignore higher order terms. The effective Hamiltonian, comprising solely of magnon modes, can be expressed as follows:

$$H_{\text{eff}}/\hbar = \sum_{j} \omega_{j} \hat{m}_{j}^{\dagger} \hat{m}_{j} + \sum_{i,j} \mathcal{G}_{ij} (\hat{m}_{i}^{\dagger} \hat{m}_{j} + \hat{m}_{i} \hat{m}_{j}^{\dagger}) \quad (10)$$

Where
$$\mathcal{G}_{ij}=g_ig_j(-1)^{|x|}(\frac{exp^{-|x|\arccos h(\Delta_i/2J)}}{2\tilde{\Delta}_i}+\frac{exp^{-|x|\arccos h(\Delta_j/2J)}}{2\tilde{\Delta}_j})$$
. Here, $x=x_i-x_j$ is the separation between ith YIG and jth YIG mode, $\tilde{\Delta}_{i,j}=\sqrt{\Delta_{i,j}^2-4J^2}$ with $\Delta_{i,j}=\omega_{i,j}-\omega_a$, and $\Delta_{i,j}$ ϵ $[-2J,2J]$ for upper and lower boundary limits of dispersion relation. Equation (10) represents a decoupled magnon with the fields, and only magnon-magnon coupling exists.

RESULTS

To illustrate the working principles of our scheme, we initially focus on a simple scenario involving an array of three cavities with N=1 (resulting in 2N+1 cavities in total, as shown in Fig. 1(a)). It is worth noting that this entanglement generation scheme remains applicable for arrays with arbitrary lengths of cavities [66]. We consider a single-mode squeezed vacuum drive applied to the YIG in the central cavity, which is located at position N+1.

We employ the quantum Langevin equations to describe the system's dynamics. By working in the frame rotating at the vacuum squeezed drive frequency ω_0 , the equations of motion take the following form (for convenience, we will omit the hat symbol from operators from now on)

$$\dot{m}_{1} = -(\kappa_{1} + i\bar{\Delta}_{1})m_{1} - i\mathcal{G}_{12}m_{2} - i\mathcal{G}_{13}m_{3} + \sqrt{2\kappa_{1}}m_{1}^{in},$$

$$\dot{m}_{2} = -(\kappa_{2} + i\bar{\Delta}_{2})m_{2} - i\mathcal{G}_{12}m_{1} - i\mathcal{G}_{23}m_{3} + \sqrt{2\kappa_{2}}m_{2}^{in},$$

$$\dot{m}_{3} = -(\kappa_{3} + i\bar{\Delta}_{3})m_{3} - i\mathcal{G}_{13}m_{1} - i\mathcal{G}_{23}m_{2} + \sqrt{2\kappa_{3}}m_{3}^{in}.$$
(11)

Here, $\bar{\Delta}_j = \omega_j + \frac{g_j^2}{2\bar{\Delta}_j}$ and $\bar{\Delta}_2 = \omega_2 - \omega_0 + \frac{g_2^2}{2\bar{\Delta}_2}$, κ_j is the dissipation rate of the magnon modes, and m_j^{in} is the input noise operator for the magnon modes. Further, the effective coupling. The separation between YIG1 and YIG2 is x=l, the same goes for YIG2 and YIG3, whereas YIG1 and YIG3 are separated by x=2l. The input noise operator m_2^{in} accounts for the driving of the central magnon mode through a squeezed vacuum field. It is characterized by zero mean and following correlation functions [82]

$$\langle m_2^{in}(t)m_2^{in\dagger}(t')\rangle = (\mathcal{N}+1)\delta(t-t'),$$

$$\langle m_2^{in\dagger}(t)m_2^{in}(t')\rangle = \mathcal{N}\delta(t-t'),$$

$$\langle m_2^{in}(t)m_2^{in}(t')\rangle = \mathcal{M}\delta(t-t'),$$

$$\langle m_2^{in\dagger}(t)m_2^{in\dagger}(t')\rangle = \mathcal{M}^*\delta(t-t').$$
(12)

Here $\mathcal{N}=\sinh^2r+\bar{n}_2(\sinh^2r+\cosh^2r)$ and $\mathcal{M}=e^{i\theta}\sinh r\cosh r(1+2\bar{n}_2)$ with θ and r being the phase and squeezing parameter of the input squeezed reservoir, respectively. In addition, \mathcal{N} and \mathcal{M} account for the number of excitations and correlations, respectively. Among these parameters, \mathcal{M} plays the most influential role in entanglement generation. The equilibrium mean thermal magnon number can be determined by $\bar{n}_2(\omega_2)=[\exp\left(\frac{\hbar\omega_2}{K_BT}\right)-1]^{-1}$.

The input noise operators for the other two magnon modes are characterized by the following correlation functions

$$\langle m_{1,3}^{in}(t)m_{1,3}^{in\dagger}(t')\rangle = (\bar{n}_{1,3} + 1)\delta(t - t'), \langle m_{1,3}^{in\dagger}(t)m_{1,3}^{in}(t')\rangle = \bar{n}_{1,3}\delta(t - t').$$
(13)

In our scheme, we showcase the possibility of generating entanglement between all potential bipartitions of the magnon modes by driving the central magnon mode with an input quantum-squeezed field. The quadratures for both the magnon modes and the input noise operators are defined as follows $x_j=(m_j+m_j^\dagger)/\sqrt{2},\ y_j=(m_j-m_j^\dagger)/\sqrt{2}i,\ \text{and}\ x_j^{in}=(m_j^{in}+m_j^{in\dagger})/\sqrt{2},\ y_j=(m_j^{in}-m_j^{in\dagger})/\sqrt{2}i,\ \text{respectively.}$ In terms of quadrature fluctuations, the quantum Langevin equation (11) can be rewritten as

$$\dot{F}(t) = F(t)A + N(t), \tag{14}$$

where $F(t)=[x_1(t),\ y_1(t),\ x_2(t),\ y_2(t),\ x_3(t),\ y_3(t)]^T$, and $N(t)=[x_1^{in}(t),\ y_1^{in}(t),\ x_2^{in}(t),\ y_2^{in}(t),\ x_3^{in}(t),\ y_3^{in}(t)]^T$ denote the quadrature fluctuation vectors of magnon and input noise operators, respectively. The drift matrix F is given by

$$F = \begin{pmatrix} -\kappa_{1} & \bar{\Delta}_{1} & 0 & \mathcal{G}_{12} & 0 & \mathcal{G}_{13} \\ -\bar{\Delta}_{1} & -\kappa_{1} & -\mathcal{G}_{12} & 0 & -\mathcal{G}_{13} & 0 \\ 0 & \mathcal{G}_{12} & -\kappa_{2} & \bar{\Delta}_{2} & 0 & \mathcal{G}_{23} \\ -\mathcal{G}_{12} & 0 & -\bar{\Delta}_{2} & -\kappa_{2} & -\mathcal{G}_{23} & 0 \\ 0 & \mathcal{G}_{13} & 0 & \mathcal{G}_{23} & -\kappa_{3} & \bar{\Delta}_{3} \\ -\mathcal{G}_{13} & 0 & -\mathcal{G}_{23} & 0 & -\bar{\Delta}_{3} & -\kappa_{3} \end{pmatrix}.$$
(15)

As the effective Hamiltonian of magnon modes, as given in Eq. (10), is quadratic, and the input quantum noise is Gaussian, as a result, the state of the system also remains Gaussian. The reduced state, consisting of three magnon modes, forms a continuous variable three-mode Gaussian state. This state can be entirely characterized by a 6×6 covariance matrix V, which is expressed as

$$V_{ij} = \frac{1}{2} \langle F_i(t) F_j(t) + F_j(t) F_i(t) \rangle \quad i, j = 1, 2, \dots, 6.$$
(16)

The steady-state solution can be obtained by solving the Lyapunov equation

$$FV + VF^T = -D (17)$$

where D is the diffusion matrix and can be derived from the noise correlation matrix; $\langle N_i(t)N_j(t)+N_j(t)N_i(t)\rangle/2=D_{ij}\delta((t-t'))$. It can be written as a direct sum of $D=D_1\oplus D_2\oplus D_3$, with $D_{1,3}=\mathrm{diag}[\kappa_{1,3}(2\bar{n}_{1,3}+1),\kappa_{1,3}(2\bar{n}_{1,3}+1)]$, and

$$D_2 = \begin{pmatrix} \kappa_2(2\mathcal{N} + 1 + \mathcal{M} + \mathcal{M}^*) & i\kappa_2(\mathcal{M}^* - \mathcal{M}) \\ i\kappa_2(\mathcal{M}^* - \mathcal{M}) & \kappa_2(2\mathcal{N} + 1 - \mathcal{M} - \mathcal{M}^*) \end{pmatrix}.$$
(18)

A. Bipartite entanglement

To investigate the entanglement between the magnon modes, we compute the logarithmic negativity \mathcal{E}_N . This quantity has

previously been proposed as a measure of entanglement and helps establish the conditions under which the two modes are entangled [83]. In the continuous variable case, the logarithmic

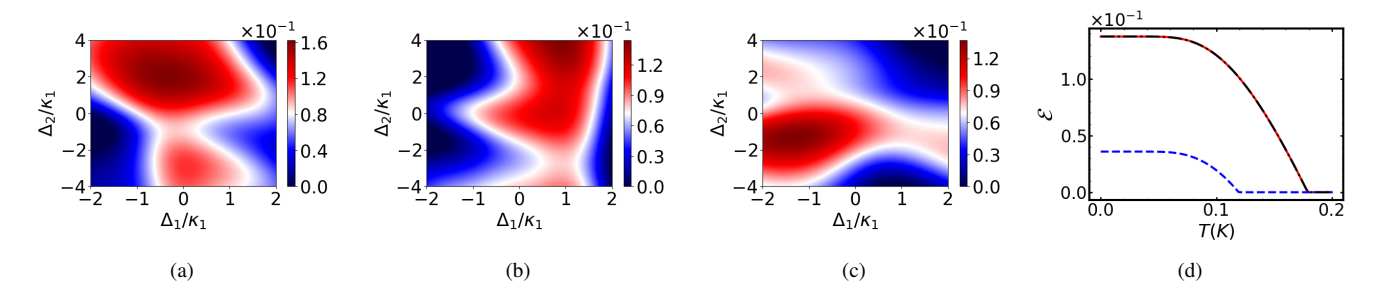


Figure 2. Density plots for logarithmic negativity between the magnon modes (a) m_1 and m_2 (b) m_2 and m_3 (c) m_1 and m_3 as a function of scaled detuning Δ_1/κ_1 and Δ_2/κ_1 . (d) Magnon-magnon bipartite entanglement $\mathcal E$ as a function of their environment temperature T. The solid, dashed, and dot-dashed lines are for $\mathcal E_{1,2}$, $\mathcal E_{1,3}$, and $\mathcal E_{2,3}$, respectively. Parameters: $\omega_j/2\pi=10$ GHz, $g_j/2\pi=20$ MHz, $J/2\pi=10$ M

negativity is defined as [84]

$$\mathcal{E} = \max[0, -\ln 2\mathcal{V}_{-}],\tag{19}$$

where $\mathcal{V}_- = \sqrt{1/2(\Sigma - (\Sigma^2 - 4\det V')^{1/2}}$ with $\Sigma = \det A + \det B - 2\det C$. V' is a 4×4 matrix obtained from steady-state covariance matrix V by removing the two rows and associated columns that are related to the traced-out magnon mode. The reduced covariance matrix V' is given by

$$V' = \begin{pmatrix} A & C \\ C^T & B \end{pmatrix}.$$

We compute the bipartite entanglement among all feasible pairs of magnon modes by employing the logarithmic negativity \mathcal{E}_N . The analytical solution of equation (17) is too cumbersome and we don't report it here. Instead, we extensively examine the logarithmic negativity across various system parameters. For numerical evaluations, we employ experimentally attainable parameters reported in recent studies [54, 85–88]. We consider the magnon density at low temperature with ground state spin s=5/2 of the Fe_3^+ ion in the YIG sphere. The total number of spins $N=\rho V$ with $\rho=4.22\times 10^{27}/m^3$ characterizing the density of each YIG and V is the volume of each sphere with diameter 250 μ -meter, this results in the total number of spins $N=3.5\times 10^6$ in each YIG.

In Fig. 2, we plot bipartite entanglement, quantified by the logarithmic negativity, between all possible pairs of magnon modes. For the results, we use a set of experimentally feasible parameters [43]: $\omega_j/2\pi = 10$ GHz, $g_j/2\pi = 20$ MHz, $J/2\pi = 10 \text{ MHz}, \kappa_1/2\pi = \kappa_3/2\pi = 5 \text{ MHz}, \kappa_3/2\pi = 10 \text{ MHz},$ r = 0.5. In Figs. 2(c-d), we assume a low temperature of T=220 mK. Without the loss of generality, we consider the input squeezed drive of zero phase $\theta = 0$. We consider identical couplings between the magnon modes, in the case of unequal interaction strengths, the entanglement becomes less. The input squeezed drive on the central magnon mode is responsible for entanglement generation between the magnon modes. The degree of entanglement decreases by reducing the squeezing parameter r, and it dies out in the absence of the squeezed drive. We observe that the difference in the order magnon decays at resonance frequencies can produce

significant changes in the amount of steady-state entanglement between the two magnon modes. Each magnon-pair has a state-swap interaction and the squeezing can be transferred from a squeezed magnon state to another magnon state. As a result, each magnon pair is to be entangled due to swap-state type interaction via squeezing. This implies that squeezing can affect the bipartite entanglement generated in between a pair of the magnon modes. The entanglement is robust against temperature and survives up to about $T=0.18~{\rm K}$ as shown in Fig. 2(d). A larger squeezing parameter r would result in more robust entanglement against environment temperature. However, we consider a moderate value of squeezing parameter r=0.5.

B. Tripartite entanglement

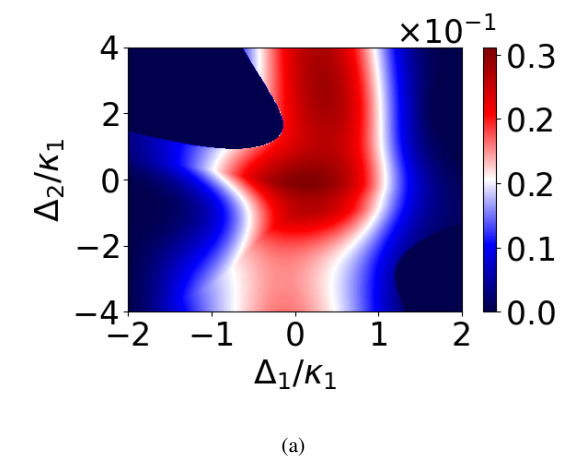
We further investigate the possibility of distant magnonmagnon tripartite entanglement generation in the array shown in Fig. 1. To this end, we employ the minimal residual contangle given by [89, 90]

$$\mathcal{R}_{i|jk} = C_{i|jk} - C_{i|j} - C_{i|k}. (20)$$

Here contangle of subsystems x and y is denoted by $C_{x|y}$, and y may represent more than one mode. $C_{x|y}$ is a proper entanglement monotone, and it is determined by the square of the logarithmic negativity between the respective modes, which is given by

$$\mathcal{E}_{i|jk} = \max[0, -\ln 2\mathcal{V}_{i|jk}],\tag{21}$$

where $\mathcal{V}_{i|jk} = \min \left| \mathrm{eig} i \Omega_3 \tilde{V} \right|$ is the smallest symplectic eigenvalues. Ω_3 is the symplectic matrix $\Omega_3 = \bigoplus_{j=1}^3 i \sigma_y$, with σ_y being the y-Pauli matrix and \oplus symbol describes the direct sum of the σ_y matrices. The 6×6 covariance matrix \tilde{V} is obtained by inverting the momentum quadrature of one of the magnon modes. The transformed covariance matrix \tilde{V} is determined by $\tilde{V} = P_{i|jk} V P_{i|jk}$ where $P_{1|23} = \mathrm{diag}[1,-1,1,1,1,1], P_{2|13} = \mathrm{diag}[1,1,1,-1,1,1],$ and $P_{3|12} = \mathrm{diag}[1,1,1,1,1,1]$ are partial transposition diagonal matrices. The steady state of the magnon modes can



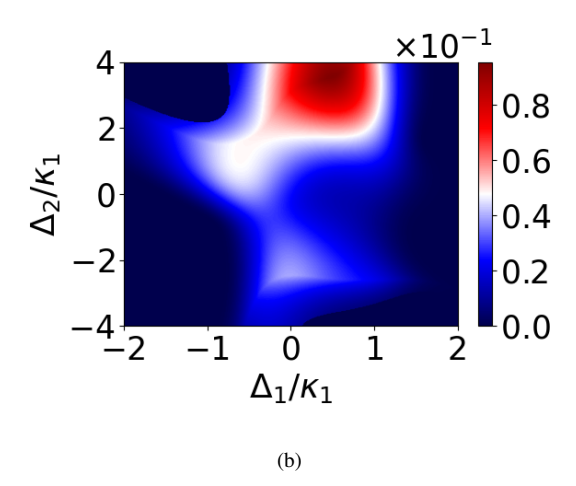


Figure 3. Two-dimensional plots for tripartite entanglement, quantified by minimal residual contangle $\mathcal R$ as a function of scaled detuning Δ_1/κ_1 and Δ_2/κ_1 . In panel (a) r=0.5, and (b) r=1, the rest of the parameters are the same as given in Fig. 2

be fully characterized by the 6×6 covariance matrix because of its Gaussian nature. The tripartite entanglement for Gaussian states can be determined by minimum residual cotangle [89, 90]

$$\mathcal{R}_{min} = min[\mathcal{R}_{1|23}, \mathcal{R}_{2|13}, \mathcal{R}_{3|12}]. \tag{22}$$

t This ensures that the tripartite entanglement remains unchanged regardless of how the modes are permuted.

Density plots of magnon-magnon tripartite entanglement determined via minimum residual cotangle \mathcal{R}_{\min} are shown in Fig. 3. It is evident from the results that considerable tripartite entanglement can be generated between magnon modes when the central magnon mode is driven by a squeezed drive. Fig. 3(b) shows that the degree of entanglement significantly enhanced with the increase in the squeezing parameter r.

V. CONCLUSION

In summary, we have shown that steady-state bipartite and tripartite entanglement can be generated between distant magnon modes when only one of these magnon modes is driven by a single-mode squeezed drive. In particular, we considered an array of N cavities each of which houses a single YIG sphere, and the central YIG is coupled to a single-mode squeezed vacuum bath. We have shown that contrary to previous proposals on magnon-magnon entanglement generation [55–63], steady-state bipartite and tripartite entanglement can be generated between the YIGs covering the whole array. The entangled pairs do not require nonlinearity, instead, entanglement is generated via a squeezed drive and its strength depends on the squeezing parameter r. The generated entanglement is robust against the environment temperature provided the magnons dissipation rates are sufficiently low. It may be interesting to look for multipartite entangled states of magnons, which is left for future works. Our work may be useful in designing quantum networks based on cavity-magnon systems [65].

VI. ACKNOWLEDGEMENT

Appendix A: Bipartite entanglement with five YIGs

Next, we extend our results for 5 YIGs (N=2), and the squeezed drive is taken on YIG3. The Langevin equations of motion are

$$\begin{split} \dot{m_{1}} &= -\left(\kappa_{1} + i\bar{\Delta}_{1}\right)m_{1} - i\sum_{i=1}^{5}\sum_{j=2}^{5}\mathcal{G}_{ij}m_{j} + \sqrt{2\kappa_{1}}m_{1_{in}},\\ \dot{m_{2}} &= -\left(\kappa_{2} + i\bar{\Delta}_{2}\right)m_{2} - i\mathcal{G}_{12}m_{1} - i\sum_{i=2}^{5}\sum_{j=3}^{5}\mathcal{G}_{ij}m_{j} +\\ &\sqrt{2\kappa_{2}}m_{2_{in}},\\ \dot{m_{3}} &= -\left(\kappa_{3} + i\bar{\Delta}_{3}\right)m_{3} - i\sum_{i=1}^{2}\sum_{j=3}\mathcal{G}_{ij}m_{i} - i\sum_{i=3}^{5}\sum_{j=4}^{5}\mathcal{G}_{ij}m_{j} +\\ &\sqrt{2\kappa_{3}}m_{3_{in}},\\ \dot{m_{4}} &= -\left(\kappa_{4} + i\bar{\Delta}_{4}\right)m_{4} - i\sum_{i=1}^{3}\sum_{j=4}\mathcal{G}_{ij}m_{i} - i\mathcal{G}_{45}m_{5} +\\ &\sqrt{2\kappa_{4}}m_{4_{in}},\\ \dot{m_{5}} &= -\left(\kappa_{5} + i\bar{\Delta}_{5}\right)m_{5} - i\sum_{i=1}^{4}\sum_{j=5}\mathcal{G}_{ij}m_{i} + \sqrt{2\kappa_{5}}m_{5_{in}}. \end{split} \tag{A1}$$

Again we write the Langevin equations in matrix form as equation (14). The A matrix is now a 10×10 matrix which can be described as

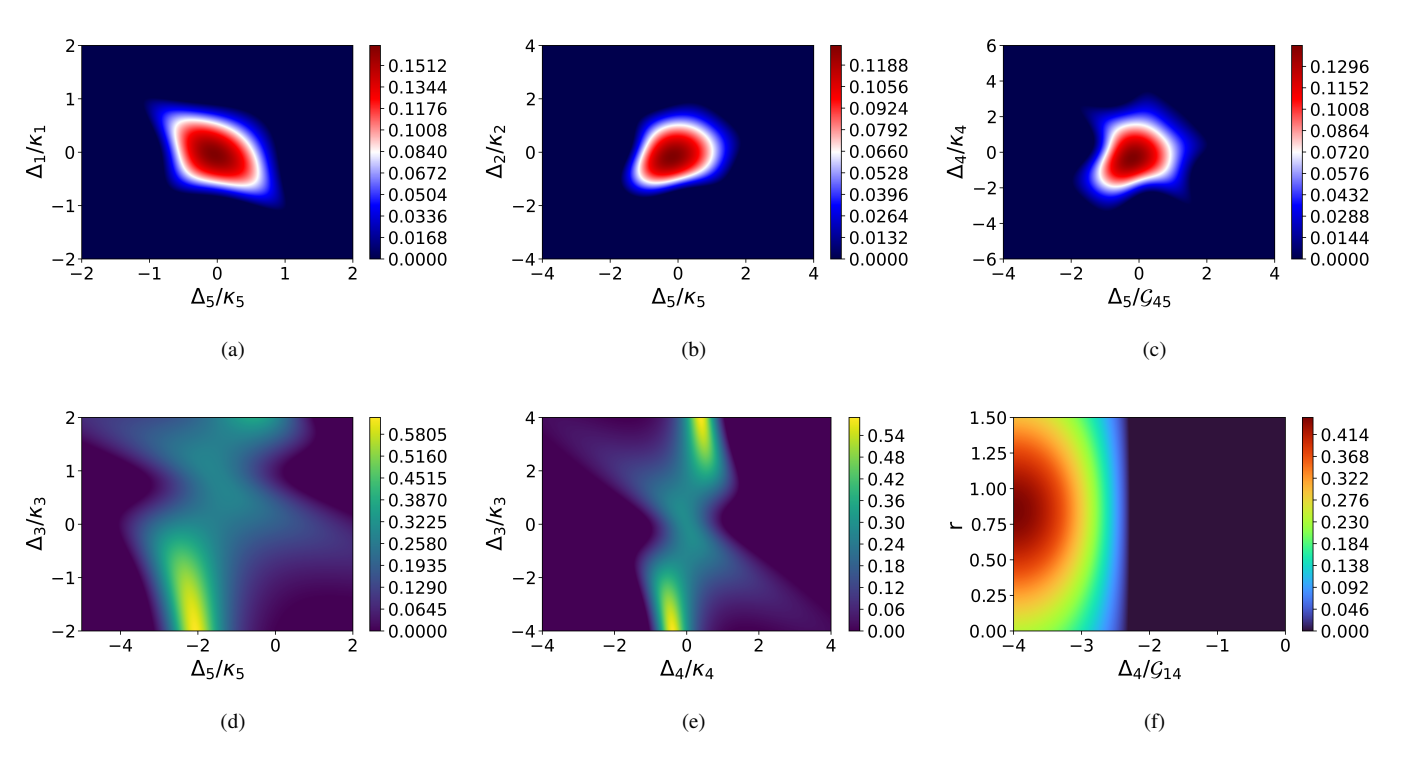


Figure 4. (Color online). In the given panel, the pairs of bipartite entanglement for a 5 YIGs sample are shown. (a) Indicates entanglement between m_1 , and m_5 modes, (b) m_2 , and m_5 , (c) m_4 , and m_5 (d) m_3 , and m_5 modes. (e) Describes the entanglement between m_3 , and m_4 , and (f) shows the squeezing effect on the entanglement between m_1 , and m_4 . In subfigures (a-e), the squeezing parameter r is taken 1.2 while other parameters remain fixed as Fig. 2

$$A = \begin{pmatrix} -\kappa_{1} & \bar{\Delta}_{1} & 0 & \mathcal{G}_{12} & 0 & \mathcal{G}_{13} & 0 & \mathcal{G}_{14} & 0 & \mathcal{G}_{15} \\ -\bar{\Delta}_{1} & -\kappa_{1} & -\mathcal{G}_{12} & 0 & -\mathcal{G}_{13} & 0 & -\mathcal{G}_{14} & 0 & -\mathcal{G}_{15} & 0 \\ 0 & \mathcal{G}_{12} & -\kappa_{2} & \bar{\Delta}_{2} & 0 & \mathcal{G}_{23} & 0 & \mathcal{G}_{24} & 0 & \mathcal{G}_{25} \\ -\mathcal{G}_{12} & 0 & -\bar{\Delta}_{2} & -\kappa_{2} & -\mathcal{G}_{23} & 0 & -\mathcal{G}_{24} & 0 & -\mathcal{G}_{25} & 0 \\ 0 & \mathcal{G}_{13} & 0 & \mathcal{G}_{23} & -\kappa_{3} & \bar{\Delta}_{3} & 0 & \mathcal{G}_{34} & 0 & \mathcal{G}_{35} \\ -\mathcal{G}_{13} & 0 & -\mathcal{G}_{23} & 0 & -\bar{\Delta}_{3} & -\kappa_{3} & -\mathcal{G}_{34} & 0 & -\mathcal{G}_{35} & 0 \\ 0 & \mathcal{G}_{14} & 0 & \mathcal{G}_{24} & 0 & \mathcal{G}_{34} & -\kappa_{4} & \bar{\Delta}_{4} & 0 & \mathcal{G}_{45} \\ -\mathcal{G}_{14} & 0 & -\mathcal{G}_{24} & 0 & -\mathcal{G}_{34} & 0 & -\bar{\Delta}_{4} & -\kappa_{4} & -\mathcal{G}_{45} & 0 \\ 0 & \mathcal{G}_{15} & 0 & \mathcal{G}_{25} & 0 & \mathcal{G}_{35} & 0 & \mathcal{G}_{45} & -\kappa_{5} & \bar{\Delta}_{5} \\ -\mathcal{G}_{15} & 0 & -\mathcal{G}_{25} & 0 & -\mathcal{G}_{35} & 0 & -\mathcal{G}_{45} & 0 & -\bar{\Delta}_{5} & -\kappa_{5}. \end{pmatrix}$$

With $F(t)=[(x_i(t), y_i(t)]^T$ and $N(t)=[x_{i_{in}}(t), y_{i_{in}}(t)]^T$ i=1,2,3,..., 10. Since the squeezed drive for N=5 is taken on YIG3, this shifts YIG3 frequency by amount of the drive frequency i.e., $\bar{\Delta}_3 = \omega_3 - \omega_0 + g_2^3/2\tilde{\Delta}_3$. We can write equation (A2) for N magnon modes in general $m \times n$ matrix form

$$Q_{ij} = \begin{pmatrix} K(\bar{\Delta}_i) & G_{ij} \\ G_{ij} & K(\bar{\Delta}_i) \end{pmatrix}$$

where,
$$K(\bar{\Delta}_i) = \begin{pmatrix} -\kappa_i & \bar{\Delta}_i \\ -\bar{\Delta}_i & -\kappa_i \end{pmatrix}$$
 and $G_{ij} = \begin{pmatrix} 0 & \mathcal{G}_{ij} \\ -\mathcal{G}_{ij} & 0 \end{pmatrix}$ for

i=1 ...N, and j=2,...are the sub-block 2×2 matrices of ith YIG decays with corresponding detuning frequency Δ_j and G_{ij} is the coupling of ith YIG with jth YIG as discussed earlier. Our model can be extended to 2N+1 cavities with a squeezed drive on N+1 YIG and can be manifested as a quantum network. The entanglement survives from YIG1 to the nth YIG due to the transfer of state from one YIG to another YIG.

- [1] F. Flamini, N. Spagnolo, and F. Sciarrino, Photonic quantum information processing: a review, Reports on Progress in Physics **82**, 016001 (2018).
- [2] T. Jennewein, C. Simon, G. Weihs, H. Weinfurter, and A. Zeilinger, Quantum cryptography with entangled photons, Phys. Rev. Lett. 84, 4729 (2000).
- [3] Y.-H. Luo, H.-S. Zhong, M. Erhard, X.-L. Wang, L.-C. Peng, M. Krenn, X. Jiang, L. Li, N.-L. Liu, C.-Y. Lu, A. Zeilinger, and J.-W. Pan, Quantum teleportation in high dimensions, Phys. Rev. Lett. 123, 070505 (2019).
- [4] R. Demkowicz-Dobrzański and L. Maccone, Using entanglement against noise in quantum metrology, Phys. Rev. Lett. 113, 250801 (2014).
- [5] S. L. Braunstein and P. van Loock, Quantum information with continuous variables, Rev. Mod. Phys. 77, 513 (2005).
- [6] B. Julsgaard, A. Kozhekin, and E. S. Polzik, Experimental long-lived entanglement of two macroscopic objects, Nature 413, 400 (2001).
- [7] C. W. Chou, H. de Riedmatten, D. Felinto, S. V. Polyakov, S. J. van Enk, and H. J. Kimble, Measurement-induced entanglement for excitation stored in remote atomic ensembles, Nature 438, 828 (2005).
- [8] R. McConnell, H. Zhang, J. Hu, S. Ćuk, and V. Vuletić, Entanglement with negative wigner function of almost 3,000 atoms heralded by one photon, Nature 519, 439 (2015).
- [9] T. A. Palomaki, J. D. Teufel, R. W. Simmonds, and K. W. Lehnert, Entangling mechanical motion with microwave fields, Science 342, 710 (2013).
- [10] C. F. Ockeloen-Korppi, E. Damskägg, J.-M. Pirkkalainen, M. Asjad, A. A. Clerk, F. Massel, M. J. Woolley, and M. A. Sillanpää, Stabilized entanglement of massive mechanical oscillators, Nature 556, 478 (2018).
- [11] S. Diehl, A. Micheli, A. Kantian, B. Kraus, H. P. Büchler, and P. Zoller, Quantum states and phases in driven open quantum systems with cold atoms, Nat. Phys. 4, 878 (2008).
- [12] F. Verstraete, M. M. Wolf, and J. Ignacio Cirac, Quantum computation and quantum-state engineering driven by dissipation, Nat. Phys. 5, 633 (2009).
- [13] H. Weimer, M. Müller, I. Lesanovsky, P. Zoller, and H. P. Büchler, A rydberg quantum simulator, Nat. Phys. 6, 382 (2010).
- [14] J. T. Barreiro, M. Müller, P. Schindler, D. Nigg, T. Monz, M. Chwalla, M. Hennrich, C. F. Roos, P. Zoller, and R. Blatt, An open-system quantum simulator with trapped ions, Nature 470, 486 (2011).
- [15] J. Cho, S. Bose, and M. S. Kim, Optical pumping into many-body entanglement, Phys. Rev. Lett. **106**, 020504 (2011).
- [16] G. Morigi, J. Eschner, C. Cormick, Y. Lin, D. Leibfried, and D. J. Wineland, Dissipative quantum control of a spin chain, Phys. Rev. Lett. 115, 200502 (2015).
- [17] F. Reiter, D. Reeb, and A. S. Sørensen, Scalable dissipative preparation of many-body entanglement, Phys. Rev. Lett. 117, 040501 (2016).
- [18] J. F. Poyatos, J. I. Cirac, and P. Zoller, Quantum reservoir engineering with laser cooled trapped ions, Phys. Rev. Lett. 77, 4728 (1996).
- [19] A. R. R. Carvalho, P. Milman, R. L. de Matos Filho, and L. Davidovich, Decoherence, pointer engineering, and quantum state protection, Phys. Rev. Lett. 86, 4988 (2001).
- [20] H. Krauter, C. A. Muschik, K. Jensen, W. Wasilewski, J. M. Petersen, J. I. Cirac, and E. S. Polzik, Entanglement generated by dissipation and steady state entanglement of two macroscopic

- objects, Phys. Rev. Lett. 107, 080503 (2011).
- [21] S. Shankar, M. Hatridge, Z. Leghtas, K. M. Sliwa, A. Narla, U. Vool, S. M. Girvin, L. Frunzio, M. Mirrahimi, and M. H. Devoret, Autonomously stabilized entanglement between two superconducting quantum bits, Nature 504, 419 (2013).
- [22] D. Kienzler, H.-Y. Lo, B. Keitch, L. de Clercq, F. Leupold, F. Lindenfelser, M. Marinelli, V. Negnevitsky, and J. P. Home, Quantum harmonic oscillator state synthesis by reservoir engineering, Science 347, 53 (2015).
- [23] J.-M. Pirkkalainen, E. Damskägg, M. Brandt, F. Massel, and M. A. Sillanpää, Squeezing of quantum noise of motion in a micromechanical resonator, Phys. Rev. Lett. 115, 243601 (2015).
- [24] M. T. Naseem and Ö. E. Müstecaplıoğlu, Ground-state cooling of mechanical resonators by quantum reservoir engineering, Commun. Phys. 4, 95 (2021).
- [25] M. T. Naseem and Özgür E Müstecaplıoğlu, Engineering entanglement between resonators by hot environment, Quantum Sci. Technol. 7, 045012 (2022).
- [26] J. I. Cirac, A. S. Parkins, R. Blatt, and P. Zoller, "dark" squeezed states of the motion of a trapped ion, Phys. Rev. Lett. 70, 556 (1993).
- [27] A. Kronwald, F. Marquardt, and A. A. Clerk, Arbitrarily large steady-state bosonic squeezing via dissipation, Phys. Rev. A 88, 063833 (2013).
- [28] Y. Tabuchi, S. Ishino, A. Noguchi, T. Ishikawa, R. Yamazaki, K. Usami, and Y. Nakamura, Quantum magnonics: The magnon meets the superconducting qubit, Comptes Rendus Physique 17, 729 (2016), quantum microwaves / Micro-ondes quantiques.
- [29] D. Lachance-Quirion, Y. Tabuchi, A. Gloppe, K. Usami, and Y. Nakamura, Hybrid quantum systems based on magnonics, Appl. Phys. Express 12, 070101 (2019).
- [30] H. Yuan, Y. Cao, A. Kamra, R. A. Duine, and P. Yan, Quantum magnonics: When magnon spintronics meets quantum information science, Phys. Rep. 965, 1 (2022), quantum magnonics: When magnon spintronics meets quantum information science.
- [31] X. Zhang, C.-L. Zou, L. Jiang, and H. X. Tang, Strongly coupled magnons and cavity microwave photons, Phys. Rev. Lett. 113, 156401 (2014).
- [32] L. Bai, M. Harder, Y. P. Chen, X. Fan, J. Q. Xiao, and C.-M. Hu, Spin pumping in electrodynamically coupled magnon-photon systems, Phys. Rev. Lett. 114, 227201 (2015).
- [33] J. Bourhill, N. Kostylev, M. Goryachev, D. L. Creedon, and M. E. Tobar, Ultrahigh cooperativity interactions between magnons and resonant photons in a yig sphere, Phys. Rev. B 93, 144420 (2016).
- [34] N. Kostylev, M. Goryachev, and M. E. Tobar, Superstrong coupling of a microwave cavity to yttrium iron garnet magnons, Applied Physics Letters 108, 10.1063/1.4941730 (2016), 062402.
- [35] X. Zhang, N. Zhu, C.-L. Zou, and H. X. Tang, Optomagnonic whispering gallery microresonators, Phys. Rev. Lett. 117, 123605 (2016).
- [36] J. A. Haigh, A. Nunnenkamp, A. J. Ramsay, and A. J. Ferguson, Triple-resonant brillouin light scattering in magneto-optical cavities, Phys. Rev. Lett. 117, 133602 (2016).
- [37] A. Osada, R. Hisatomi, A. Noguchi, Y. Tabuchi, R. Yamazaki, K. Usami, M. Sadgrove, R. Yalla, M. Nomura, and Y. Nakamura, Cavity optomagnonics with spin-orbit coupled photons, Phys. Rev. Lett. 116, 223601 (2016).
- [38] J. T. Hou and L. Liu, Strong coupling between microwave photons and nanomagnet magnons, Phys. Rev. Lett. 123, 107702 (2019).

- [39] Y. Li, T. Polakovic, Y.-L. Wang, J. Xu, S. Lendinez, Z. Zhang, J. Ding, T. Khaire, H. Saglam, R. Divan, J. Pearson, W.-K. Kwok, Z. Xiao, V. Novosad, A. Hoffmann, and W. Zhang, Strong coupling between magnons and microwave photons in on-chip ferromagnet-superconductor thin-film devices, Phys. Rev. Lett. 123, 107701 (2019).
- [40] I. A. Golovchanskiy, N. N. Abramov, V. S. Stolyarov, M. Weides, V. V. Ryazanov, A. A. Golubov, A. V. Ustinov, and M. Y. Kupriyanov, Ultrastrong photon-to-magnon coupling in multi-layered heterostructures involving superconducting coherence via ferromagnetic layers, Science Advances 7, eabe8638 (2021).
- [41] Y.-P. Wang, G.-Q. Zhang, D. Zhang, X.-Q. Luo, W. Xiong, S.-P. Wang, T.-F. Li, C.-M. Hu, and J. Q. You, Magnon kerr effect in a strongly coupled cavity-magnon system, Phys. Rev. B 94, 224410 (2016).
- [42] D. Zhang, X.-Q. Luo, Y.-P. Wang, T.-F. Li, and J. Q. You, Observation of the exceptional point in cavity magnon-polaritons, Nat. Commun. 8, 1368 (2017).
- [43] X. Zhang, C.-L. Zou, L. Jiang, and H. X. Tang, Cavity magnomechanics, Science Advances 2, e1501286 (2016).
- [44] K. Ullah, M. T. Naseem, and O. E. Müstecaplıoğlu, Tunable multiwindow magnomechanically induced transparency, fano resonances, and slow-to-fast light conversion, Phys. Rev. A 102, 033721 (2020).
- [45] Y.-P. Wang, G.-Q. Zhang, D. Zhang, T.-F. Li, C.-M. Hu, and J. Q. You, Bistability of cavity magnon polaritons, Phys. Rev. Lett. 120, 057202 (2018).
- [46] G.-Q. Zhang and J. Q. You, Higher-order exceptional point in a cavity magnonics system, Phys. Rev. B 99, 054404 (2019).
- [47] C. Kong, H. Xiong, and Y. Wu, Magnon-induced nonreciprocity based on the magnon kerr effect, Phys. Rev. Appl. 12, 034001 (2019).
- [48] Z.-X. Liu, H. Xiong, and Y. Wu, Magnon blockade in a hybrid ferromagnet-superconductor quantum system, Phys. Rev. B 100, 134421 (2019).
- [49] J. Li, S.-Y. Zhu, and G. S. Agarwal, Squeezed states of magnons and phonons in cavity magnomechanics, Phys. Rev. A 99, 021801 (2019).
- [50] S. Sharma, V. A. S. V. Bittencourt, A. D. Karenowska, and S. V. Kusminskiy, Spin cat states in ferromagnetic insulators, Phys. Rev. B 103, L100403 (2021).
- [51] F.-X. Sun, S.-S. Zheng, Y. Xiao, Q. Gong, Q. He, and K. Xia, Remote generation of magnon schrödinger cat state via magnonphoton entanglement, Phys. Rev. Lett. 127, 087203 (2021).
- [52] H. Y. Yuan, P. Yan, S. Zheng, Q. Y. He, K. Xia, and M.-H. Yung, Steady bell state generation via magnon-photon coupling, Phys. Rev. Lett. 124, 053602 (2020).
- [53] Z.-B. Yang, H. Jin, J.-W. Jin, J.-Y. Liu, H.-Y. Liu, and R.-C. Yang, Bistability of squeezing and entanglement in cavity magnonics, Phys. Rev. Res. 3, 023126 (2021).
- [54] J. Li, S.-Y. Zhu, and G. S. Agarwal, Magnon-photon-phonon entanglement in cavity magnomechanics, Phys. Rev. Lett. 121, 203601 (2018).
- [55] D.-W. Luo, X.-F. Qian, and T. Yu, Nonlocal magnon entanglement generation in coupled hybrid cavity systems, Opt. Lett. 46, 1073 (2021).
- [56] Z. Zhang, M. O. Scully, and G. S. Agarwal, Quantum entanglement between two magnon modes via kerr nonlinearity driven far from equilibrium, Phys. Rev. Res. 1, 023021 (2019).
- [57] J. Li and S.-Y. Zhu, Entangling two magnon modes via magnetostrictive interaction, New J. Phys. 21, 085001 (2019).
- [58] J. M. P. Nair and G. S. Agarwal, Deterministic quantum entanglement between macroscopic ferrite samples, Applied Physics Letters 117, 10.1063/5.0015195 (2020).

- [59] Q. Zheng, W. Zhong, G. Cheng, and A. Chen, Genuine magnonphoton-magnon tripartite entanglement in a cavity electromagnonical system based on squeezed-reservoir engineering, Quantum Information Processing 22, 140 (2023).
- [60] D. Zhao, W. Zhong, G. Cheng, and A. Chen, Controllable magnon–magnon entanglement and one-way epr steering with two cascaded cavities, Quantum Inf. Processing 21, 384 (2022).
- [61] M. Yu, S.-Y. Zhu, and J. Li, Macroscopic entanglement of two magnon modes via quantum correlated microwave fields, J. Phys. B: At. Mol. Opt. Phys. 53, 065402 (2020).
- [62] W.-J. Wu, Y.-P. Wang, J.-Z. Wu, J. Li, and J. Q. You, Remote magnon entanglement between two massive ferrimagnetic spheres via cavity optomagnonics, Phys. Rev. A 104, 023711 (2021).
- [63] Y.-l. Ren, J.-k. Xie, X.-k. Li, S.-l. Ma, and F.-l. Li, Long-range generation of a magnon-magnon entangled state, Phys. Rev. B 105, 094422 (2022).
- [64] J.-Y. Liu, J.-W. Jin, X.-M. Zhang, Z.-G. Zheng, H.-Y. Liu, Y. Ming, and R.-C. Yang, Distant entanglement generation and controllable information transfer via magnon–waveguide systems, Results in Physics 52, 106854 (2023).
- [65] J. Li, Y.-P. Wang, W.-J. Wu, S.-Y. Zhu, and J. You, Quantum network with magnonic and mechanical nodes, PRX Quantum 2, 040344 (2021).
- [66] S. Zippilli, J. Li, and D. Vitali, Steady-state nested entanglement structures in harmonic chains with single-site squeezing manipulation, Phys. Rev. A 92, 032319 (2015).
- [67] A. Bienfait, P. Campagne-Ibarcq, A. H. Kiilerich, X. Zhou, S. Probst, J. J. Pla, T. Schenkel, D. Vion, D. Esteve, J. J. L. Morton, K. Moelmer, and P. Bertet, Magnetic resonance with squeezed microwaves, Phys. Rev. X 7, 041011 (2017).
- [68] Y. Tabuchi, S. Ishino, A. Noguchi, T. Ishikawa, R. Yamazaki, K. Usami, and Y. Nakamura, Coherent coupling between a ferromagnetic magnon and a superconducting qubit, Science 349, 405 (2015).
- [69] D. Porras and J. J. García-Ripoll, Shaping an itinerant quantum field into a multimode squeezed vacuum by dissipation, Phys. Rev. Lett. 108, 043602 (2012).
- [70] W. Zhang, D.-Y. Wang, C.-H. Bai, T. Wang, S. Zhang, and H.-F. Wang, Generation and transfer of squeezed states in a cavity magnomechanical system by two-tone microwave fields, Opt. Express 29, 11773 (2021).
- [71] J. Li, Y.-P. Wang, J.-Q. You, and S.-Y. Zhu, Squeezing microwaves by magnetostriction, National Science Review 10, nwac247 (2022), https://academic.oup.com/nsr/article-pdf/10/5/nwac247/50426152/nwac247.pdf.
- [72] J. Zhao, Y. Liu, L. Wu, C.-K. Duan, Y.-x. Liu, and J. Du, Observation of anti-PT-symmetry phase transition in the magnon-cavity-magnon coupled system, Phys. Rev. Appl. 13, 014053 (2020).
- [73] H. Fröhlich, Theory of the superconducting state. i. the ground state at the absolute zero of temperature, Phys. Rev. **79**, 845 (1950).
- [74] S. Nakajima, Perturbation theory in statistical mechanics, Advances in Physics 4, 363 (1955).
- [75] S. Bravyi, D. P. DiVincenzo, and D. Loss, Schrieffer-wolff transformation for quantum many-body systems, Annals of Physics 326, 2793 (2011).
- [76] S. Ma, M. J. Woolley, I. R. Petersen, and N. Yamamoto, Pure gaussian states from quantum harmonic oscillator chains with a single local dissipative process, J. Phys. A: Math. Theor. 50, 135301 (2017).
- [77] Y. Yanay and A. A. Clerk, Reservoir engineering with localized dissipation: Dynamics and prethermalization, Phys. Rev. Res. 2,

- 023177 (2020).
- [78] S. Zippilli and D. Vitali, Dissipative engineering of gaussian entangled states in harmonic lattices with a single-site squeezed reservoir, Phys. Rev. Lett. **126**, 020402 (2021).
- [79] J. Angeletti, S. Zippilli, and D. Vitali, Dissipative stabilization of entangled qubit pairs in quantum arrays with a single localized dissipative channel, Quantum Sci. Technol. 8, 035020 (2023).
- [80] J. M. Luttinger and W. Kohn, Motion of electrons and holes in perturbed periodic fields, Phys. Rev. 97, 869 (1955).
- [81] J. R. Schrieffer and P. A. Wolff, Relation between the anderson and kondo hamiltonians, Phys. Rev. 149, 491 (1966).
- [82] C. W. Gardiner, Inhibition of atomic phase decays by squeezed light: A direct effect of squeezing, Phys. Rev. Lett. 56, 1917 (1986).
- [83] G. Vidal and R. F. Werner, Computable measure of entanglement, Phys. Rev. A **65**, 032314 (2002).
- [84] G. Adesso, A. Serafini, and F. Illuminati, Extremal entanglement and mixedness in continuous variable systems, Phys. Rev. A 70, 022318 (2004).

- [85] Y. Tabuchi, S. Ishino, T. Ishikawa, R. Yamazaki, K. Usami, and Y. Nakamura, Hybridizing ferromagnetic magnons and microwave photons in the quantum limit, Phys. Rev. Lett. 113, 083603 (2014).
- [86] M. E. Kimchi-Schwartz, L. Martin, E. Flurin, C. Aron, M. Kulkarni, H. E. Tureci, and I. Siddiqi, Stabilizing entanglement via symmetry-selective bath engineering in superconducting qubits, Phys. Rev. Lett. 116, 240503 (2016).
- [87] X. Zhang, C.-L. Zou, L. Jiang, and H. X. Tang, Cavity magnomechanics, Science advances 2, e1501286 (2016).
- [88] R.-C. Shen, J. Li, Z.-Y. Fan, Y.-P. Wang, and J. Q. You, Mechanical bistability in kerr-modified cavity magnomechanics, Phys. Rev. Lett. 129, 123601 (2022).
- [89] G. Adesso and F. Illuminati, Continuous variable tangle, monogamy inequality, and entanglement sharing in gaussian states of continuous variable systems, New J. Phys. 8, 15 (2006).
- [90] G. Adesso and F. Illuminati, Entanglement in continuousvariable systems: recent advances and current perspectives, J. Phys. A: Math. Theor. 40, 7821 (2007).